Markers of NETosis and DAMPs are altered in critically ill COVID-19 patients

Joram Huckriede
Universiteit Maastricht Cardiovascular Research Institute Maastricht
Sara Bülow Anderberg
Uppsala Universitet
Albert Morales
Institut d'Investigacions Biomediques de Barcelona
Femke de Vries
Universiteit Maastricht Cardiovascular Research Institute Maastricht
Michael Hultström
Uppsala Universitet
Anders Bergqvist
Uppsala Universitet
José T. Ortiz
Hospital Clinic Barcelona
Jan Willem Sels
Maastricht Universitair Medisch Centrum+
Kanin Wichapong
Universiteit Maastricht Cardiovascular Research Institute Maastricht
Miklos Lipcsey
Uppsala Universitet
Marcel van de Poll
Maastricht Universitair Medisch Centrum+
Anders Larsson
Uppsala Universitet
Tomas Luther
Uppsala Universitet
Chris Reutelingsperger
Universiteit Maastricht Cardiovascular Research Institute Maastricht
Pablo Garcia de Frutos
Institut d'Investigacions Biomediques de Barcelona
Robert Frithiof
Uppsala Universitet
Gerry A.F. Nicolaes (g.nicolaes@maastrichtuniversity.nl)

Universiteit Maastricht Cardiovascular Research Institute Maastricht https://orcid.org/0000-0002-2482-0412

Research

Keywords: Covid-19, ARDS, Intensive care unit, NETosis, histones, cell free DNA, GAS6, sAXL, neutrophil elastase, mortality

DOI: https://doi.org/10.21203/rs.3.rs-52432/v1

Abstract

Background Coronavirus disease 19 (COVID-19) is known to present with disease severities of varying degree. In its most severe form, infection may lead to respiratory failure and multi-organ dysfunction. Here we study the levels of extracellular histone H3 (H3), neutrophil elastase (NE) and cfDNA in relation to other plasma parameters, including the immune modulators GAS6 and AXL, ICU scoring systems and mortality in patients with severe COVID-19.

Methods We measured plasma H3, NE, cfDNA, GAS6 and AXL concentration in plasma of 83 COVID-19-positive and 11 COVID-19-negative patients at admission to the Intensive Care Unit (ICU) at the Uppsala University hospital, a tertiary hospital in Sweden and a total of 333 samples obtained from these patients during the ICU-stay. We determined their correlation with disease severity, organ failure, mortality and other blood parameters.

Results H3, NE, cfDNA, GAS6 and AXL were increased in plasma of COVID-19 patients compared to controls. cfDNA and GAS6 decreased in time in in patients surviving to 30 days post ICU admission. Plasma H3 was a common feature of COVID-19 patients, detected in 40% of the patients at ICU admission. Although these measures were not predictive of the final outcome of the disease, they correlated well with parameters of tissue damage (H3 and cfDNA) and neutrophil counts (NE). A subset of samples displayed H3 processing, possibly due to proteolysis.

Conclusions Elevated H3 and cfDNA levels in COVID-19 patients illustrate the severity of the cellular damage observed in critically ill COVID-19 patients. The increase in NE indicates the important role of neutrophil response and the process of NETosis in the disease. GAS6 appears as part of an early activated mechanism of response in Covid-19.

Background

In severe cases, COVID-19 disease develops into an acute respiratory distress syndrome (ARDS), an acute lung injury causing patients to be dependent of ventilator support, which may be accompanied by development of multiple organ failure (MOF) [1]. Mortality appears is seen primarily in patients over the age of 65 [2–5] and is highest for infected individuals with underlying comorbidities such as hypertension, cardiovascular disease or diabetes [6–8]. For patients who are taken into the intensive care unit (ICU), a high SOFA score and increased levels of fibrin D-dimers have been reported [9] to associate with poor prognosis. Mild thrombocytopenia (platelet counts $< 150 \times 10^9$ cells per L) can be found in 70–95% of patients with severe COVID-19 [10, 11], but does not appear to be an important predictor of disease progression or adverse outcome [11, 12]. However, 35–45% of COVID-19 patients develop thromboembolic complications that contribute to the overall clinical prognosis [13], a much higher proportion than the 5–15% usually seen in critically ill patients [14–16]. These coagulopathies include thrombotic microangiopathies and disseminated intravascular coagulation (DIC). The observed symptoms are reminiscent of bacterial sepsis but COVID-19 has distinct features [17] given the relatively

mild reduction in platelet count and high values of D-dimer seen in COVID-19, pointing at a somewhat different pathological mechanism. The involvement of immune regulatory and hemostatic pathways appears evident.

Given the systemic infection and activation of the innate immune system in severe COVID-19 patients and the organ injury, in particular in the lungs, cellular components released upon cellular disruption or neutrophil activation may contribute to COVID-19 disease. This is in line with the observation that in the acute respiratory distress syndrome, the involvement of the innate immune systems' neutrophil extracellular traps, NETs was previously shown to occur and to contribute to disease progress [18].

Extracellular histones are cytotoxic proteins that originate from the activation of neutrophils during NETosis [19–21] or from damaged tissues [22], while cell free DNA (cfDNA) and the protease neutrophil elastase (NE) are released concomitantly [23]. Histones and cfDNA, are known to activate Toll-like receptors (TLRs) and promote proinflammatory cytokine release via receptor-dependent and independent pathways [24, 25]. Extracellular histones and NE have antimicrobial activities and aid in the killing of pathogens. However, while serving a protective function, NETs are potentially harmful to the host. NET formation in lung tissue is able to disturb microcirculation and NETs can easily expand in pulmonary alveoli, filling the lungs [26], while it was seen that histones can rapidly and strongly accumulate in the lung capillary network [27].

Histones have been shown to activate and recruit leukocytes [28], damage alveolar macrophages [29], activate erythrocytes [30], epithelial and endothelial cells, in particular pulmonary endothelial cells [31–33]. Collectively, extracellular histones cause an inflammatory response that leads to microvascular leakage and endothelial dysfunction, inducing an immunothrombotic procoagulant condition and eventually organ failure. If not cleared from circulation, histones as well as cfDNA facilitate severe systemic inflammation and worsen the clinical condition [34, 35]. In a previous study [36] we reported a correlation with mortality of the plasma concentration of extracellular histone H3 in sepsis patients admitted to the ICU. Presence of NE in plasma is associated with exacerbations, lung function decline and disease severity in patients with COPD, bronchiectasis and cystic fibrosis [37–39] and decrease of NE levels in bronchiectasis patients improved lung function and airway inflammation [40].

At the same time that it provides a first line of defense against infections, the innate immune system initiates self-control responses to prevent damage to the host. One system involved in early immunomodulation is the GAS6/TAM ligand/receptor system [41]. GAS6 is a vitamin K-dependent protein that activates the TAM family (Tyro3, AXL and MerTK) of tyrosine kinase membrane receptors [42]. The GAS6/TAM system regulates the immune response by modulating cytokine production, inducing a regulatory cellular response profile and by mediating efferocytosis, removing irreversibly damaged cells. The system also provides a mechanism of regulating endothelial and platelet activation and interaction [43].

Extracellular histones and cfDNA are implicated in regulation of inflammatory and hemostatic pathways in the context of severe viral infections and ARDS, all of which are implicated in COVID-19. Therefore, the

objective of this study was to determine circulating levels of extracellular histone H3, cfDNA, NE, and components of the GAS6/TAM system in a group of 83 consecutive patients admitted to an intensive care unit (ICU) and compare them with pre-COVID-19 UCI patients (n = 11) and healthy controls (n = 15).

Materials And Methods

Subjects and sampling

The study was approved by the Swedish National Ethical Review Agency (EPM; No. 2020 – 01623). Informed consent was obtained from the patient, or next of kin if the patient was unable give consent. The Declaration of Helsinki and its subsequent revisions were followed. The protocol of the study was registered (ClinicalTrials ID: NCT04316884).

All adult patients with confirmed or suspected COVID-19 admitted to the ICU between March 21, and April 13, 2020 were screened for eligibility. The diagnosis was established by PCR detection of SARS-CoV-2 E and N-genes in nasopharyngealswabs according to previously described protocols [44]. Plasma samples were collected from 83 consecutive patients. We further used 11 previously included ICU-patients without COVID-19 as ICU-controls and included 15 healthy control subjects who were healthy university employed volunteers.

For a subset of patients, longitudinal plasma samples were available (n = 22), taken between days 1 and 12, which allowed analysis of time-dependent development of plasma values for the markers measured. For other patients, longitudinal sampling could not be performed due to mortality and/or limitations in logistic capacity at the peak of ICU occupancy.

The first blood sample (in citrate buffer) collected after a patient was admitted to the ICU was used as baseline measurement. Platelet poor plasma (PPP) was prepared by centrifugation of the blood for 10 min at 3000 g at 4 ºC, after which the supernatant was carefully pipetted, whilst taking care not to disturb the cell-containing lower layer by keeping a generous margin from the buffy coat. PPP was aliquoted and snap-frozen until use. The healthy control PPP was prepared by the same method as the patient plasma.

Quantitation of cell-free DNA

Cell-free DNA (cfDNA) was quantitated from plasma essentially as described earlier [45] using a real-time PCR-based assay. In short, plasma samples were diluted 8-fold in water to result in a final assay dilution of 40 times. Reactions were performed in 96-well plates (Roche) employing a LightCycler 480 qPCR machine (Roche). Reaction volumes contained 5 µL of TATAA Probe GrandMaster Mix/no ROX (TATAA Biocenter), 0.5 µL TATAA Alu-60 assay probes (TATAA Biocenter), 2.5 µL H2O and 2 µL of sample. Amplification consisted of a pre-denaturation step 2 minutes at 95 °C, to activate the DNA Polymerase in the master mix. Followed by 40 cycles of denaturation at 95 °C for 5 s, annealing at 60 °C for 10 s and extension at 60 °C for 30 s. A calibration range (from 1 to 300 ng/µL) using purified and quantitated DNA

standard prepared as described [46] was included in each analysis, facilitating the direct correlation of Ct values to DNA concentration.

Quantitation of NE, sAXL, and GAS6 in Plasma

NE, soluble AXL (sAXL), and GAS6 levels in plasma were determined by the ELISA technique using commercial kits from R&D systems (DuoSet ELISA, Bio-techne, Minneapolis, USA) according to the manufacturer's instructions. For determination of sAXL, the plasma form of the AXL cellular receptor, and GAS6, plasma samples were diluted 1:40 and 1:200 for NE. All samples were determined in duplicates.

Analysis of extracellular histone H3

Extracellular histone H3 levels were determined using a semi-quantitative method previously described [36, 47]. Briefly, plasma dilutions were subjected to SDS-PAGE gel electrophoresis and transferred to PVDF membranes (Bio-Rad Laboratories, Hemel Hempstead, UK) using semi-dry blotting. Membranes were blocked and incubated with primary anti-H3 antibody, o/n at 4 °C, (sc-8654-R, Santa Cruz Biotechnology, Heidelberg, Germany), followed by a secondary biotin-conjugated IgG for 30 minutes at RT (ab97083, Abcam, Cambridge, UK) and a streptavidin-biotin/alkaline phosphatase complex (Vectastain ABC-Alkaline Phosphatase for 30 min at RT, Vector Laboratories, Burlingame, USA). Histone H3 bands were detected by luminescent ECL substrate (Advansta, San Jose, USA). Resulting band densities were quantified by ImageQuant TL software (GE Healtcare, Little Chalfont, UK), as compared to known concentrations of purified calf thymus H3 (Roche, Basel, Switzerland). This analysis is independent of frequently observed cross reactivity of histone antibodies with non-histone plasma proteins and allows the inspection of potential *in vivo* histone proteolytic processing. The detection of citrullinated histone H3 was performed on a subset of 50 randomly selected COVID-19 patients that had verified presence of H3 and used an anti-citrulline antibody to inspect the presence of citrullinated protein at an overlaying position at 15 kDa employing the anti-citrulline detection kit (Part number 17- 347B-1) and the monoclonal antibody (MABS487, Merck) in combination with a polyclonal anti-human IgGHRP-labelled antibody (DAKO, P0214). Imaging was performed as described for the histone H3 analysis described above.

Statistical analysis

Graphpad Prism version 8 (Graphpad Software Inc., La Jolla, CA, USA) and SPSS Statistics version 26 (SPSS Inc., Chicago, IL, USA) were used for statistical analysis. We employed a Kolmogorov-Smirnov test to inspect normality of data. Parametric data are presented as mean (SD) or geometric mean (95% CI) for log-transformed data unless stated. Non-parametric data are presented as median and inter quartile range (IQR). We used paired and unpaired t-test and one-way analysis of variance (ANOVA) to compare variables. Mann-Whitney tests were used for comparison of groups. *** indicates $p < 0.001$.

Results

Of all ICU patients included, 83 patients had a confirmed COVID-19 diagnosis and 11 patients did not have COVID-19 and were used as ICU control patients. We obtained a total of 315 plasma-samples from the 83 patients with confirmed COVID-19, while 18 samples from 11 patients were obtained from the ICU control group. The healthy control group consisted of 15 individuals with a median age of 32 (IQR 24–37) of which 7 were male (47%).

The baseline (day 1) characteristics of the 83 ICU patients are shown in Table 1. Between the COVID-19 and the non-COVID-19 patients, males were overrepresented in the infected group, with 71.1% ($p = 0.030$), whereas BMI was not different between both ICU groups. Non-COVID-19 patients tended to be older than the COVID-19 patients. To allow comparison with a healthy population, a healthy control group was further included in our analyses.

Table 1

Demographic and baseline characteristics of 94 patients on admission to the Intensive Care Unit. Values are represented as median (IQR) or n (%).The p-value is calculated for continuous parameters with the Mann-Whitney U test, and for categorical parameters the chi-square test; $p < 0.05$ is considered significant.

	ICU Covid-19 **n = 83**	**ICU Control** **n = 11**	***P***
Age, yrs, median	60 (52–71)	70 (59–75)	0.193
Gender, male N	59 (71)	5 (46)	0.030
BMI	28.8 (25.1–32.7)	27.7 (25.4–31.8)	0.829
Respiratory rate, breaths/min	27 (22–35)	15 (15–17)	0.001
Heart rate, beats/min	88 (77–100)	80 (72–92)	0.208
MAP, mmHg	90 (81–98)	80 (67–86)	0.004
Temperature, °C	38.0 (37.4–38.7)	36.4 (36.4–36.7)	< 0.001
Diabetes, yes	22 (27)	2 (18)	0.552
Hypertension, yes	41 (50)	4 (36)	0.375
Heart failure, yes	3 (4)	1 (9)	0.398
Ischemic heart failure, yes	8 (10)	0 (0)	0.282
Vessel disease, yes	12 (15)	1 (9)	0.628
Malignancy, yes	4 (5)	11 (100)	< 0.001
HIPEC surgery, yes	0 (0)	11 (100)	< 0.001
Pulmonary disease, yes	21 (25)	1 (9)	0.233
Asthma	14 (17)	1 (9)	
COPD	6 (7)		
Sarcoidosis	1 (1)		
Smoker No	67 (80.7)	9 (81.8)	0.721
Yes	3 (3.6)	0 (0)	
Previous	10 (12.0)	2 (18.2)	
Unknown	3 (3.6)		
Steroid treatment, yes	9 (11)	1 (9)	0.850
ACEi/ARB treatment, yes	29 (35)	2 (18)	0.256

	ICU Covid-19 n = 83	ICU Control n = 11	*P*
Anticoagulant treatment, yes	16 (19)	5 (46)	0.050
SAPS-3	52 (47–58)	54 (49–58)	0.568
SOFA	6 (4–8)	6 (6–8)	0.980

Physiological characteristics are also shown in Table 1. Between the COVID-19 and the non-COVID-19 patients, significant differences were observed in their clinical parameters, with respiratory rate, mean arterial pressure (MAP) and body temperature being higher in the COVID-19 group.

Prior to ICU admittance, malignancy, representing the main indication for ICU admission for HIPEC surgery of the non-COVID-19 group and anticoagulant treatment were significantly higher in the control ICU group ($p < 0.001$ and $p\ 0.050$ respectively). All patients in both patient groups required supplemental inspired oxygen (Supplemental Table 1), but in the ICU control patients no high-flow nasal oxygen (HFNO) or oxygen masks were required, yet the latter group received more vasoactive treatment. No significant differences were present in antibiotic use. Supplementary Tables 2 and 3 presents routine parameters measured for most COVID-19 patients at study inclusion. The PaO2/FiO2 ratio, a clinical indicator of respiratory dysfunction, was on average 149 mmHg (IQR 123–186 mmHg) in the COVID-19 group. Leukocytes were increased in the ICU control patients whereas erythrocytes and thrombocytes were within reference range for both patient groups. A significant rise in CRP, IL-6 (n = 40), procalcitonin, and lactate dehydrogenase (LDH) was seen in the COVID-19 patients, indicative of the ongoing inflammatory response and tissue damage. All these measures had the lower interquartile range above the reference range. D-dimer, indicative of fibrinolytic activation, was also above the reference range, although in the 19 patients where aPTT was measured, the median value was prolonged but within reference range.

Detection of Histone H3, cfDNA and NE in plasma.

Plasma samples from the 94 ICU patients, were analyzed together with those of 15 healthy volunteers (Fig. 1). In the majority of patients (67%), no extracellular H3 could be detected at ICU admission. As compared with plasma samples of the ICU control patients however, the levels of extracellular histone H3 in the COVID-19 patients on day 1 were significantly higher ($p = 0.047$), as well as compared to the healthy controls ($p = 0.025$; Fig. 1A), while there was no significant difference between the ICU control and healthy control group (Table 2). The cfDNA values from both ICU groups differ greatly ($p < 0.001$), with the COVID-19 group presenting 25-times higher levels than of the control group (Fig. 1B). The levels of cfDNA did not differ between the ICU control and healthy control patients (Table 2). There was a highly significant difference between both groups when NE was determined ($p < 0.001$; Fig. 1C) with NE being virtually absent from the ICU control group and the healthy controls (Table 2).

Table 2
Baseline ICU patients and healthy control plasma parameters expressed as median (IQR).

		ICU COVID-19 n = 83	ICU Control n = 11	Healthy Control n = 15	*P*
Histone H3	*µg/ml*	0.0 (0.0–0.3)	0.0 (0.0–0.0)	0.0 (0.0–0.0)	0.004
cfDNA	*ng/µl*	225.8 (125.7–456.3)	7.8 (5.9–17.1)	4.1 (2.8–5.3)	< 0.001
Gas6	*ng/ml*	24.8 (18.1–33.3)	12.1 (9.5–15.9)	14.4 (11.0–19.7)	< 0.001
sAxl	*ng/ml*	19.8 (14.6–26.1)	13.2 (11.3–17.6)	17.3 (13.7–18.4)	0.018
NE	*ng/ml*	71.9 (32.4–134.9)	0.0 (0.0–0.0)	0.0 (0.0–0.0)	< 0.001
P-values were calculated with the Kruskal-Wallis test with Dunn's post-hoc test.					

Detection of GAS6 and sAXL in plasma.

In COVID-19 and non-COVID-19 ICU patients, the GAS6 concentration at study inclusion was 24.8 (18.1–33.3) ng/mL and 12.1 (9.5–15.9) ng/mL respectively, indicating a significant difference between both groups ($p < 0.001$; Fig. 2A, Table 2). The concentration of the healthy control group 14.4 (11.0–19.7) ng/mL is significantly lower ($p < 0.001$) compared to the COVID-19 ICU group, while no difference is found with the non-COVID-19 ICU group (Table 2).

The concentration of sAXL at inclusion between the ICU groups being 19.8 (14.6–26.1) ng/mL and 13.2 (11.3–17.6) ng/mL respectively, showed a significant increase ($p < 0.001$) of the COVID-19 group compared to the non-COVID-19. The concentration of the healthy controls 17.3 (13.7–18.5) ng/mL was lower than that of the COVID-19 group, though this difference was not significant.

Correlations between different plasma markers and laboratory parameters.

Table 3
Correlations between various parameters measured at day 1.

	N	Correlation	*P*
H3 vs. cfDNA	83	0.367	0.001
H3 vs. sAXL	83	0.245	0.026
H3 vs. NE	83	0.391	< 0.001
cfDNA vs. Leukocytes	79	0.235	0.037
cfDNA vs. Platelets	79	0.236	0.036
cfDNA vs AST	67	0.262	0.032
cfDNA vs. LDH	64	0.506	< 0.001
sAXL vs. Troponin I	65	0.355	0.004
GAS6 vs. Procalcitonin	72	0.246	0.038
Correlations were calculated with the Spearman's rank-order correlation test. Correlations were considered significant if $P < 0.05$, only significant correlations are mentioned here.			

The concentration of H3 correlated with cfDNA and NE concentrations at ICU admission in COVID-19 patients (Table 3). At this point, there was no significant correlation between cfDNA and NE measurements. In contrast, LDH correlated very well with cfDNA (0.506; $p < 0.001$), which could indicate a common origin in cellular damage. Remarkably, sAXL correlated significantly with the myocardial injury biomarker troponin I in this cohort.

These correlations persisted when all subsequent sampling was included (supplementary Table 4). In addition, other correlations with biochemical parameters indicating organ damage were observed, including H3 and cfDNA with AST, LDH and procalcitonin (weaker for H3 in the latter case; $p = 0.029$). Interestingly, cfDNA correlated also with D-dimer and CRP when all points were considered, indicators of ongoing coagulation and fibrinolysis. Although NE correlated strongly with H3 as was the case with the initial values, NE did not correlate significantly with other tissue damage parameters, nor with cfDNA, while it correlated significantly with leukocyte and neutrophil cell count, as well as procalcitonin and GAS6 (Supplementary Table 4).

Prognosis and time-dependent parameter development in COVID-19.

At ICU admission, the value of SAPS-3 score (but not SOFA, supplementary Fig. 1) was significantly higher in the group of COVID-19 patients that did not survive (n = 21) compared to those that survived (n = 62; supplementary Table 5). Non-survivors were older, hypertensive (86%), and had vessel or ischemic heart failure more frequently than survivors. Accordingly, they were more frequently treated with

anticoagulants and ACEi/ARB treatment. They also suffered more thromboembolisms during ICU stay. From the biochemical measurements performed, non-survivors had higher markers of organ damage, including AST, troponin I and procalcitonin (Supplementary Table 6). In those patients where IL-6 was determined, mean IL-6 concentration in non-survivors (n = 10) was almost 3 times that of survivors (n = 30). Although cfDNA, H3, NE, sAXL and GAS6 were all elevated in COVID-19 positive patients at admission, none of these parameters was a good predictor of final outcome. Indeed, at ICU admission, there was no correlation of any of these parameters with SAPS-3 or SOFA scores.

In 22 patients where several samples could be obtained during their ICU stay, we studied the time-dependent development of the markers. We arbitrarily divided the results in an early sample (day 1–5) and a late sample (day 6–12), using the mean value of the different samples obtained during each period (supplementary Table 7). Platelet counts, in the normal range in the baseline measurements, increased significantly in the late samples, as well as leukocytes (supplementary Table 7). Markers of tissue damage also increased, including ALT and AST. There were no significant differences between early and late values of histone H3, cfDNA or NE, although more samples were positive for H3 in the latter group. No differences were observed for sAXL or GAS6. We furthermore inspected if the correlations observed in the initial samples persisted over the early (day 1–5) and late phase of ICU stay for the 22 COVID-19 patients for which data were available over this complete period of time (Supplementary Table 8). We observed that H3 correlated with cfDNA over both time periods and generally showed persistent correlation with neutrophil counts. Strong correlations were seen between NE levels and neutrophils (0,810 and 0,708 respectively for early and late phase).

Next, we divided the 22 patients according to their final outcome at 30 days (Fig. 3). Those individuals that survived (n = 15) showed a 40% decrease in cfDNA concentration in the late plasma samples. Further, in these patients GAS6 concentration decreased more than 30% in late samples. In contrast, neither cfDNA nor GAS6 decreased in the group of non-survivors (n = 7), with their late values being very similar to the early ones. The same trends were observed in H3 and NE measurements, although in these cases, it did not reach significance. In addition, when regarding the NE concentrations, we found both in the early phase, and in the late phase a significant difference between survivors and non-survivors.

Histone Analysis

Extracellular histone H3 was detected exclusively in samples originating from COVID-19 patients. At ICU admission, 27 out of 83 COVID-19 positive patients (33%) had detectable histone H3 in plasma. When considered the whole group of 315 samples obtained at different time points, histones were detected in 135 (43%) samples obtained from 83 patients.

Table 4
Comparison of histone positive and histone negative samples.

	Histone Positive (n = 135)	Histone Negative (n = 180)	*P*
Histone Cleavage	55 (40.7%)	0 (0%)	
Histone H3 (µg/ml)	0.59 (0.14–1.39)	0.00 (0.00–0.00)	< 0.001
NE (ng/ml)	98.6 (60.0–159.0)	53.5 (19.6–109.6)	< 0.001
cfDNA (ng/µl)	555.0 (321.9–829.6)	244.8 (137.7–429.1)	< 0.001

Cleavage of Histone H3 and Plasma levels of Histone H3, NE and cfDNA in all samples of COVID-19 patients (n = 315), expressed as median (IQR). Samples are stratified in two groups depending on histone H3 presence. P-value is calculated with the Mann-Whitney U test; $p < 0.05$ is considered significant.

Histone positive samples contained significantly higher NE and cfDNA than those in which no H3 was detected ($p < 0,001$ and $p < 0,001$ respectively, Table 4), in line with the strong correlation between these parameters (Table 3 and supplementary table 4). The presence of histone in COVID-19 patients appeared not randomly divided over time (Fig. 3). Although no statistical significance was reached for comparison between early and late survivors/non-survivors, the average histone levels in early survivors were higher than in late survivors, whereas average histone H3 levels in early non-survivors were lower than in late non-survivors.

In several COVID-19 patients, histone H3 showed an additional 13 kDa band on Western blot (Figs. 4A and 4B). This was seen in 37% of histone H3 positive patients at day 1 and overall in 40,7% of all samples tested. The origin of this band is most likely a proteolytic cleavage of the single 15 kDa band. In one patient, only the lower weight band was seen (patient 47, day 7, Fig. 4A), suggesting full H3 proteolysis. In 5 patients, the proteolysis disappeared in samples collected after 6 days or later of ICU stay.

In addition to presence of histones per se, we found that in a subset of 50 randomly selected COVID-19 patients with histone H3 in their plasma, the presence of citrullinated histone and found that 36 of these (72%) were positive for citrullination (Fig. 4C).

Discussion

Our study broadly assessed a series of biomarkers reflecting the process of cellular damage and NETosis as well as a mechanism of early response to damage, the GAS6/AXL pathway, in a group of severely ill patients, consecutively admitted at an ICU during the present COVID-19 pandemic. A non-COVID-19 group was included consisting of ICU patients suffering from malignancies requiring surgery (Supplementary Table 1). PaO2/FiO2 ratios were clearly lower in the COVID-19 group, resulting in higher percentage of

invasive respiration applied. Increased tissue damage, and particularly lung tissue damage, with more pronounced inflammation, in combination with pulmonary thromboembolic disease could explain this difference. This is underscored by increases in CRP, IL-6, D-dimer, LDH, procalcitonin, ASAT and increased neutrophil counts at admission (Supplementary Table 2).

Levels of cfDNA, H3 and NE differed significantly already at admission to ICU care between the COVID-19 and non-COVID-19 groups. This is likely indicative of increased tissue damage and neutrophil activation in this group. Given the equimolar presence of core histones H1, H2A, H2B, H3 and H4 in nucleosomes, exposure of H3 to the extracellular milieu, is equally indicative for presence of the other core histones. However, histones H3 and H4 have been found to be the most toxic [21, 48]. While cfDNA and NE levels appeared to decrease over time, we noted that when analyzing the full collection of H3 measured, the highest levels of histones were found for the days 4–8 and that this marker was on average less present during the first days of ICU admission. Given the difference to NE and the at least partial NETosis origin of H3 (as indicated by their citrullination) we hypothesize that a rapid clearance of histone H3 in the early phase of ICU stay could explain the observed overall lower levels of circulating free histone H3. The clearance of cytotoxic histones could represent a protective response that is brought about by uptake by immune cells, binding to intact glycocalyx or binding to endothelium, platelets, or vesicles that originate from these cells. Even though more data are required to support our hypothesis, the latter could contribute to the observed reduction in platelet counts and, by virtue of their capacity to activate endothelium and platelets, to the observed increase in thromboembolic events. Remarkably, we noted that in a sub-set of plasma samples that contained H3, exclusively found in the COVID-19 group, H3 was proteolyzed. Several proteases are known to process extracellular histones including NE. Partial processing of H3 by NE was shown to occur during NET formation [49]. Given the observed correlation between H3 proteolysis and NE levels, we conclude that in COVID-19 patients, extracellular histones are most likely processed by NE. Of note, we realize the limitations of the semi-quantitative H3 assay used here, mostly being time-intensive, however, unless truly specific antibodies are available, proteolysis would be undetected using commonly applied solid-phase based methods like ELISA.

We further found that in a subset of 50 histone H3 containing samples, histone H3 was citrullinated in 36 (72%), suggesting that histone exposure involves the activity of PAD4 as is the case during ROS-independent NETosis. It is likely that the non-citrullinated H3 originates from damaged tissue or from PAD4-independent NETosis pathways.

It has been suggested that cfDNA could serve as a surrogate marker for NETosis in critically ill mechanically ventilated patients in whom NETs contribute to local alveolar inflammation [50]. However, our data show that cfDNA correlated best with H3, while the correlation with NE was less strong. This could indicate that NET formation could be better reflected by the release of neutrophil-specific markers such as NE, while H3 and cfDNA could relate to cellular damage in a broader sense. cfDNA is a DAMP able to activate TLRs. The sustained increase in cfDNA observed in COVID-19 patients would propagate inflammation through TLR activation. In this sense, it is important to stress that cfDNA decreased over time in those patients that survived the infection, while those that did not survive maintained constantly

high plasma cfDNA concentrations. Likewise, increased levels of NE are able to reduce the lung permeability barrier function and induce release of pro-inflammatory cytokines, collectively inducing emphysematous lesions.

We observed H3 positive samples levels at ICU admission, like we found earlier in a critically ill ICU population of sepsis patients[36]. While this points at similar pathways being involved in disease onset and progression, other reports [51] pointed out that COVID-19 clinical features are similar but different from those seen in sepsis. The observed normal platelet counts found in most samples in this study, irrespective of the phase of the disease or its outcome, further underscore this point. A possible early onset of NETosis, with an associated rise in extracellular histones is supported by our observation that NE levels were evident already from day 1 till day 12, implying neutrophil activation and NETosis, accompanied by cfDNA also being present already at day 1.

The components of the GAS6/TAM system have been shown to increase in a diverse spectrum of inflammatory conditions [52], including sepsis and septic shock; but also systemic inflammatory response syndrome (SIRS) without infection [53]. In several studies, GAS6 concentration in plasma at IC admission correlated with severity of organ damage, either in SOFA or with damage of specific organs [53–57]. This also the case in viral infections. Using a murine model of respiratory syncytial virus (RSV) infection, Shibata et al [58] showed that GAS6 is expressed upon infection in lung alveoli, leading to conversion of alveolar macrophages into M2-like cells. These studies illustrate the modulatory role of the innate response provided by the GAS6/TAM system and suggest that the presence of these components in plasma could be an early event in the orchestration of the immune response to viral infections.

In our COVID-19 cohort, GAS6 concentrations at ICU admission more than doubled those of non-COVID-19 IC patients. Among plasma determinations that correlate with GAS6 are the interleukins IL-6 [53, 54] and IL-8 [54]. GAS6, IL-6 and IL-8 concentrations are increased in septic patients who develop acute lung injury (ALI; [53). Plasma GAS6 concentration was able to significantly discriminate patients that would develop ALI in that cohort {Yeh, 2017 #63]. Also, non-survivors of sepsis in ICU tend to have initial higher concentration of GAS6 and GAS6 could predict mortality with an AUC of 0.7 [54]. However, in our cohort, no evident correlation with severity of the lung symptoms could be established, which could reflect a specific characteristic of SARS-CoV-2 interaction with the system.

In our study group, GAS6 concentration was maximal at IC admission, and was maintained high in non-survivors. Ni et al have shown that recombinant GAS6 infusion improves the outcome of experimental sepsis in mice, controlling multi-organ dysfunction [59]. One of the target cells of GAS6 in bacterial infection is the vascular endothelium, that showed reduced LPS-induced permeability in the presence of GAS6. Interestingly, GAS6 is also necessary to maintain the response of vascular endothelium during inflammatory conditions, allowing endothelial cell interactions with platelets and leukocytes [43].

While the concentration of sAXL was found increased in sepsis cohorts [53, 54], the increase was not so evident and did not significantly correlate with organ damage, similarly to our observation in COVID-19 patients. Soluble AXL is an ADAM-shed form of the receptor, found in plasma in a complex with GAS6

[60]. The specific increase of GAS6 over sAXL in COVID-19 could reflect a need of free, active GAS6 in this condition. Interestingly, sAXL showed a correlation with troponin I. This reflects the observed correlation of sAXL with parameters and progression of heart failure also observed in previous studies [61], and could indicate a specific implication of AXL in the cardiac damage observed in COVID-19. It is possible that in the context of COVID-19, GAS6 could be acting through another TAM receptor in this context, MerTK. MerTK inhibition increases the inflammatory cytokine storm in LPS-induced ALI [62], acting as a tolerogenic receptor under inflammatory conditions [63]. However, it has to be noted that LPS and other PAMPs drastically reduce MerTK expression [63].

Conclusion

We have shown the presence of extracellular histone H3 and cfDNA in the plasma of COVID-19 patients to be significantly different from plasma of ICU patients who did not have COVID-19. Cytotoxic extracellular histone H3 was found in 40% of COVID-19 patients, theoretically contributing to disease progress, but not predicting final disease outcome. Histones were found to correlate with parameters for tissue damage and with neutrophil counts, implying their partial origin from NETosis. This was supported by the observation of cfDNA that showed a strong correlation with extracellular histone levels, suggesting their possible use as proxy markers for the assessment of plasma histone levels. In COVID-19, an early activation of the GAS6 immunomodulatory pathway takes place, reflected in a clear increase of the plasma concentration of this vitamin K dependent protein.

Of the markers tested, development of neutrophil elastase proofed significantly different in COVID-19 survivors, as compared to non-survivors, with NE levels showing a decrease over time in survivors as opposed to an increase in non-survivors, again supporting the important role that neutrophils play in this disease. The involvement of NETosis and DAMPS in COVID-19 provides a possible rational basis for treatment options that are able to target NETosis or its associated cytotoxic and pro-inflammatory DAMPS in support of existing therapies in the ICU.

List Of Abbreviations

ACEi/ARB – angiotensin converting enzyme inhibitors/angiotensin-receptor blockers; ADAM – a disintegrin and metalloproteinase; ALI - acute lung injury; ALT – alanine transaminase; APTT - activated partial thromboplastin time; ARDS – acute respiratory distress syndrome; AST – aspartate aminotransferase; AUC – area under the curve; AXL – AXL receptor tyrosine kinase; BMI – body mass index; cfDNA – cellular free deoxynucleic acid; COPD - chronic obstructive pulmonary disease; COVID-19 – Coronavirus Disease 19; CRP – C-reactive protein; DAMP – damage associated molecular pattern; DIC – disseminated intravascular coagulation; eGFR – estimated glomerular filtration rate; ELISA – enzyme-linked immunoassay; Gas6 – growth arrest-specific 6; HFNO – high flow nasal oxygen; HIPEC – hyperthermic intraperitoneal chemotherapy; HRP – horseradish peroxidase; ICU – intensive care unit; IgG – immunoglobin G; IL-6 – interleukin 6; IL-8 – interleukin 8; IQR – interquartile range; kDa – kilodalton; LDH – lactate dehydrogenase; LPS – lipopolysaccharide; MAP – mean arterial pressure; MOF – multiple

organ failure; NE – neutrophil elastase; NET – neutrophil extracellular trap; PAD4 – peptidyl arginine deiminase 4; PAMP – pathogen associated molecular pattern; PaO2/FiO2 – partial pressure of arterial oxygen/fraction of inspired oxygen; PCR – polymerase chain reaction; PPP – platelet poor plasma; PVDF – polyvinylidene fluoride; RSV – respiratory syncytial virus; SAPS-3 – simplified acute physiology score; SARS-CoV-2 – severe acute respiratory syndrome coronavirus 2; SDS-PAGE – sodium dodecyl sulfate-polyacrylamide gel electrophoresis; SIRS – systemic inflammatory response syndrome; SOFA – sequential organ failure assessment; TAM – Tyro3-Axl-Mer; TLR – Toll like receptor

Declarations

Ethics approval and consent to participate

The study was approved by the Swedish National Ethical Review Agency (EPM; No. 2020-01623). Informed consent was obtained from the patient, or next of kin if the patient was unable give consent. The Declaration of Helsinki and its subsequent revisions were followed. The protocol of the study was registered (ClinicalTrials ID: NCT04316884).

Consent for publication

Not applicable.

Availability of data and materials

The data used and/or analyzed in the present study are available from the corresponding author on reasonable request.

Competing interests

Not applicable

Funding

The study was supported through grants from the dedSciLifeLab/KAW national COVID-19 research program project grant (MH), by Scilifelab, the Knut and Alice Wallenberg Foundation and in part by the Swedish Research Council (RF, grant no 2014-02569 and 2014-07606), and the Netherlands Thrombosis Foundation (GN).

Authors contributions

GAFN and RF contributed equally to this work. All authors participated in conception and design of the study. RF, SB, MH, ML, AL, AB and TL participated in data collection, analysis and interpretation. JH and FV performed and analyzed the experiments. KW, CR, MP, JWS, AM, JTO contributed to supervision and data analysis and provided intellectual input. RF and PGF contributed to funding. GAFN drafted the

manuscript, provided funding, performed experiments and analyzed data. All authors contributed to manuscript revision and gave approval of the final version.

Acknowledgements

We would like to thank Mrs. Gwen Keulen for technical assistance and Mr. René van Oerle for providing study material. We thank Research nurses Joanna Wessbergh and Elin Söderman, and biobank assistants Philip Karlsson and Erik Danielsson for their expertise in compiling the study.

References

1. Pedersen SF, Ho YC: SARS-CoV-2: a storm is raging. *J Clin Invest* 2020.
2. Novel Coronavirus Pneumonia Emergency Response Epidemiology T: [The epidemiological characteristics of an outbreak of 2019 novel coronavirus diseases (COVID-19) in China]. *Zhonghua Liu Xing Bing Xue Za Zhi* 2020, 41(2):145-151.
3. Onder G, Rezza G, Brusaferro S: Case-Fatality Rate and Characteristics of Patients Dying in Relation to COVID-19 in Italy. *JAMA* 2020.
4. COVID-19-Associated Hospitalizations by age
5. Richardson S, Hirsch JS, Narasimhan M, Crawford JM, McGinn T, Davidson KW, and the Northwell C-RC, Barnaby DP, Becker LB, Chelico JD *et al*: Presenting Characteristics, Comorbidities, and Outcomes Among 5700 Patients Hospitalized With COVID-19 in the New York City Area. *JAMA* 2020.
6. Guan WJ, Liang WH, Zhao Y, Liang HR, Chen ZS, Li YM, Liu XQ, Chen RC, Tang CL, Wang T *et al*: Comorbidity and its impact on 1590 patients with COVID-19 in China: a nationwide analysis. *Eur Respir J* 2020, 55(5).
7. Zaki N, Alashwal H, Ibrahim S: Association of hypertension, diabetes, stroke, cancer, kidney disease, and high-cholesterol with COVID-19 disease severity and fatality: A systematic review. *Diabetes Metab Syndr* 2020, 14(5):1133-1142.
8. WHO Director-General's statement on the advice of the IHR Emergency Committee on Novel Coronavirus, January 23rd 2020
9. Zhou F, Yu T, Du R, Fan G, Liu Y, Liu Z, Xiang J, Wang Y, Song B, Gu X *et al*: Clinical course and risk factors for mortality of adult inpatients with COVID-19 in Wuhan, China: a retrospective cohort study. *Lancet* 2020, 395(10229):1054-1062.
10. Guan WJ, Ni ZY, Hu Y, Liang WH, Ou CQ, He JX, Liu L, Shan H, Lei CL, Hui DSC *et al*: Clinical Characteristics of Coronavirus Disease 2019 in China. *N Engl J Med* 2020, 382(18):1708-1720.
11. Huang C, Wang Y, Li X, Ren L, Zhao J, Hu Y, Zhang L, Fan G, Xu J, Gu X *et al*: Clinical features of patients infected with 2019 novel coronavirus in Wuhan, China. *Lancet* 2020, 395(10223):497-506.
12. Wada H, Thachil J, Di Nisio M, Mathew P, Kurosawa S, Gando S, Kim HK, Nielsen JD, Dempfle C-E, Levi M *et al*: Guidance for diagnosis and treatment of disseminated intravascular coagulation from harmonization of the recommendations from three guidelines. *J Thromb Haemost* 2020, 11:761-767.

13. Tang N, Li D, Wang X, Sun Z: Abnormal coagulation parameters are associated with poor prognosis in patients with novel coronavirus pneumonia. *J Thromb Haemost* 2020, 18(4):844-847.
14. Klok FA, Kruip M, van der Meer NJM, Arbous MS, Gommers D, Kant KM, Kaptein FHJ, van Paassen J, Stals MAM, Huisman MV *et al*: Confirmation of the high cumulative incidence of thrombotic complications in critically ill ICU patients with COVID-19: An updated analysis. *Thromb Res* 2020.
15. Klok FA, Kruip M, van der Meer NJM, Arbous MS, Gommers D, Kant KM, Kaptein FHJ, van Paassen J, Stals MAM, Huisman MV *et al*: Incidence of thrombotic complications in critically ill ICU patients with COVID-19. *Thromb Res* 2020.
16. Group PIftCCCT, the A, New Zealand Intensive Care Society Clinical Trials G, Cook D, Meade M, Guyatt G, Walter S, Heels-Ansdell D, Warkentin TE, Zytaruk N *et al*: Dalteparin versus unfractionated heparin in critically ill patients. *N Engl J Med* 2011, 364(14):1305-1314.
17. Levi M, Scully M: How I treat disseminated intravascular coagulation. *Blood* 2018, 131(8):845-854.
18. Wong JJM, Leong JY, Lee JH, Albani S, Yeo JG: Insights into the immuno-pathogenesis of acute respiratory distress syndrome. *Ann Transl Med* 2019, 7(19):504.
19. Brinkmann V, Reichard U, Goosmann C, Fauler B, Uhlemann Y, Weiss DS, Weinrauch Y, Zychlinsky A: Neutrophil extracellular traps kill bacteria. *Science* 2004, 303(5663):1532-1535.
20. Fuchs TA, Brill A, Duerschmied D, Schatzberg D, Monestier M, Myers DD, Jr., Wrobleski SK, Wakefield TW, Hartwig JH, Wagner DD: Extracellular DNA traps promote thrombosis. *Proc Natl Acad Sci U S A* 2010, 107(36):15880-15885.
21. Silvestre-Roig C, Braster Q, Wichapong K, Lee EY, Teulon JM, Berrebeh N, Winter J, Adrover JM, Santos GS, Froese A *et al*: Externalized histone H4 orchestrates chronic inflammation by inducing lytic cell death. *Nature* 2019, 569(7755):236-240.
22. Zeerleder S, Zwart B, Wuillemin WA, Aarden LA, Groeneveld AB, Caliezi C, van Nieuwenhuijze AE, van Mierlo GJ, Eerenberg AJ, Lammle B *et al*: Elevated nucleosome levels in systemic inflammation and sepsis. *Crit Care Med* 2003, 31(7):1947-1951.
23. Dau T, Sarker RS, Yildirim AO, Eickelberg O, Jenne DE: Autoprocessing of neutrophil elastase near its active site reduces the efficiency of natural and synthetic elastase inhibitors. *Nat Commun* 2015, 6:6722.
24. Rock KL, Latz E, Ontiveros F, Kono H: The sterile inflammatory response. *Annu Rev Immunol* 2010, 28:321-342.
25. Silk E, Zhao H, Weng H, Ma D: The role of extracellular histone in organ injury. *Cell Death Dis* 2017, 8(5):e2812.
26. Porto BN, Stein RT: Neutrophil Extracellular Traps in Pulmonary Diseases: Too Much of a Good Thing? *Front Immunol* 2016, 7:311.
27. Freeman CG, Parish CR, Knox KJ, Blackmore JL, Lobov SA, King DW, Senden TJ, Stephens RW: The accumulation of circulating histones on heparan sulphate in the capillary glycocalyx of the lungs. *Biomaterials* 2013, 34(22):5670-5676.

28. Nowak D, Piasecka G, Hrabec E: Chemotactic activity of histones for human polymorphonuclear leukocytes. *Exp Pathol* 1990, 40(2):111-116.
29. Sun M, Jiang X, Jin Y, Yang H, Chen C, Lyu X, Wen Z: [Extracellular histones are involved in lipopolysaccharide-induced alveolar macrophage injury by activating the TWIK2-NLRP3 pathway]. *Zhonghua Wei Zhong Bing Ji Jiu Yi Xue* 2020, 32(2):194-198.
30. Kordbacheh F, O'Meara CH, Coupland LA, Lelliott PM, Parish CR: Extracellular histones induce erythrocyte fragility and anemia. *Blood* 2017, 130(26):2884-2888.
31. Abrams ST, Zhang N, Manson J, Liu T, Dart C, Baluwa F, Wang SS, Brohi K, Kipar A, Yu W *et al*: Circulating histones are mediators of trauma-associated lung injury. *Am J Respir Crit Care Med* 2013, 187(2):160-169.
32. Collier DM, Villalba N, Sackheim A, Bonev AD, Miller ZD, Moore JS, Shui B, Lee JC, Lee FK, Reining S *et al*: Extracellular histones induce calcium signals in the endothelium of resistance-sized mesenteric arteries and cause loss of endothelium-dependent dilation. *Am J Physiol Heart Circ Physiol* 2019, 316(6):H1309-H1322.
33. Zhang Y, Guan L, Yu J, Zhao Z, Mao L, Li S, Zhao J: Pulmonary endothelial activation caused by extracellular histones contributes to neutrophil activation in acute respiratory distress syndrome. *Respir Res* 2016, 17(1):155.
34. Meng W, Paunel-Gorgulu A, Flohe S, Hoffmann A, Witte I, MacKenzie C, Baldus SE, Windolf J, Logters TT: Depletion of neutrophil extracellular traps in vivo results in hypersusceptibility to polymicrobial sepsis in mice. *Crit Care* 2012, 16(4):R137.
35. Camicia G, Pozner R, de Larranaga G: Neutrophil extracellular traps in sepsis. *Shock* 2014, 42(4):286-294.
36. Wildhagen KC, Wiewel MA, Schultz MJ, Horn J, Schrijver R, Reutelingsperger CP, van der Poll T, Nicolaes GA: Extracellular histone H3 levels are inversely correlated with antithrombin levels and platelet counts and are associated with mortality in sepsis patients. *Thromb Res* 2015, 136(3):542-547.
37. Thulborn SJ, Mistry V, Brightling CE, Moffitt KL, Ribeiro D, Bafadhel M: Neutrophil elastase as a biomarker for bacterial infection in COPD. *Respir Res* 2019, 20(1):170.
38. Chalmers JD, Moffitt KL, Suarez-Cuartin G, Sibila O, Finch S, Furrie E, Dicker A, Wrobel K, Elborn JS, Walker B *et al*: Neutrophil Elastase Activity Is Associated with Exacerbations and Lung Function Decline in Bronchiectasis. *Am J Respir Crit Care Med* 2017, 195(10):1384-1393.
39. Muhlebach MS, Clancy JP, Heltshe SL, Ziady A, Kelley T, Accurso F, Pilewski J, Mayer-Hamblett N, Joseloff E, Sagel SD: Biomarkers for cystic fibrosis drug development. *J Cyst Fibros* 2016, 15(6):714-723.
40. Stockley R, De Soyza A, Gunawardena K, Perrett J, Forsman-Semb K, Entwistle N, Snell N: Phase II study of a neutrophil elastase inhibitor (AZD9668) in patients with bronchiectasis. *Respir Med* 2013, 107(4):524-533.

41. van der Meer JH, van der Poll T, van 't Veer C: TAM receptors, Gas6, and protein S: roles in inflammation and hemostasis. *Blood* 2014, 123(16):2460-2469.
42. Lemke G: Phosphatidylserine Is the Signal for TAM Receptors and Their Ligands. *Trends Biochem Sci* 2017, 42(9):738-748.
43. Tjwa M, Bellido-Martin L, Lin Y, Lutgens E, Plaisance S, Bono F, Delesque-Touchard N, Herve C, Moura R, Billiau AD *et al*: Gas6 promotes inflammation by enhancing interactions between endothelial cells, platelets, and leukocytes. *Blood* 2008, 111(8):4096-4105.
44. Corman VM, Landt O, Kaiser M, Molenkamp R, Meijer A, Chu DK, Bleicker T, Brunink S, Schneider J, Schmidt ML *et al*: Detection of 2019 novel coronavirus (2019-nCoV) by real-time RT-PCR. *Euro Surveill* 2020, 25(3).
45. Breitbach S, Tug S, Helmig S, Zahn D, Kubiak T, Michal M, Gori T, Ehlert T, Beiter T, Simon P: Direct quantification of cell-free, circulating DNA from unpurified plasma. *PLoS One* 2014, 9(3):e87838.
46. Xue X, Teare MD, Holen I, Zhu YM, Woll PJ: Optimizing the yield and utility of circulating cell-free DNA from plasma and serum. *Clin Chim Acta* 2009, 404(2):100-104.
47. van Smaalen TC, Beurskens DM, Hoogland ER, Winkens B, Christiaans MH, Reutelingsperger CP, van Heurn LW, Nicolaes GA: Presence of Cytotoxic Extracellular Histones in Machine Perfusate of Donation After Circulatory Death Kidneys. *Transplantation* 2017, 101(4):e93-e101.
48. Xu J, Zhang X, Pelayo R, Monestier M, Ammollo CT, Semeraro F, Taylor FB, Esmon NL, Lupu F, Esmon CT: Extracellular histones are major mediators of death in sepsis. *Nat Med* 2009, 15(11):1318-1321.
49. Papayannopoulos V, Metzler KD, Hakkim A, Zychlinsky A: Neutrophil elastase and myeloperoxidase regulate the formation of neutrophil extracellular traps. *J Cell Biol* 2010, 191(3):677-691.
50. Mikacenic C, Moore R, Dmyterko V, West TE, Altemeier WA, Liles WC, Lood C: Neutrophil extracellular traps (NETs) are increased in the alveolar spaces of patients with ventilator-associated pneumonia. *Crit Care* 2018, 22(1):358.
51. Levi M, Thachil J, Iba T, Levy JH: Coagulation abnormalities and thrombosis in patients with COVID-19. *Lancet Haematol* 2020.
52. Salmi L, Gavelli F, Patrucco F, Caputo M, Avanzi GC, Castello LM: Gas6/TAM Axis in Sepsis: Time to Consider Its Potential Role as a Therapeutic Target. *Dis Markers* 2019, 2019:6156493.
53. Ekman C, Linder A, Akesson P, Dahlback B: Plasma concentrations of Gas6 (growth arrest specific protein 6) and its soluble tyrosine kinase receptor sAxl in sepsis and systemic inflammatory response syndromes. *Crit Care* 2010, 14(4):R158.
54. Stalder G, Que YA, Calzavarini S, Burnier L, Kosinski C, Ballabeni P, Roger T, Calandra T, Duchosal MA, Liaudet L *et al*: Study of Early Elevated Gas6 Plasma Level as a Predictor of Mortality in a Prospective Cohort of Patients with Sepsis. *PLoS One* 2016, 11(10):e0163542.
55. Yeh LC, Huang PW, Hsieh KH, Wang CH, Kao YK, Lin TH, Lee XL: Elevated Plasma Levels of Gas6 Are Associated with Acute Lung Injury in Patients with Severe Sepsis. *Tohoku J Exp Med* 2017, 243(3):187-193.

56. Gibot S, Massin F, Cravoisy A, Dupays R, Barraud D, Nace L, Bollaert PE: Growth arrest-specific protein 6 plasma concentrations during septic shock. *Crit Care* 2007, 11(1):R8.
57. Borgel D, Clauser S, Bornstain C, Bieche I, Bissery A, Remones V, Fagon JY, Aiach M, Diehl JL: Elevated growth-arrest-specific protein 6 plasma levels in patients with severe sepsis. *Crit Care Med* 2006, 34(1):219-222.
58. Shibata T, Makino A, Ogata R, Nakamura S, Ito T, Nagata K, Terauchi Y, Oishi T, Fujieda M, Takahashi Y *et al*: Respiratory syncytial virus infection exacerbates pneumococcal pneumonia via Gas6/Axl-mediated macrophage polarization. *J Clin Invest* 2020.
59. Ni J, Lin M, Jin Y, Li J, Guo Y, Zhou J, Hong G, Zhao G, Lu Z: Gas6 Attenuates Sepsis-Induced Tight Junction Injury and Vascular Endothelial Hyperpermeability via the Axl/NF-kappaB Signaling Pathway. *Front Pharmacol* 2019, 10:662.
60. Ekman C, Stenhoff J, Dahlback B: Gas6 is complexed to the soluble tyrosine kinase receptor Axl in human blood. *J Thromb Haemost* 2010, 8(4):838-844.
61. Batlle M, Campos B, Farrero M, Cardona M, Gonzalez B, Castel MA, Ortiz J, Roig E, Pulgarin MJ, Ramirez J *et al*: Use of serum levels of high sensitivity troponin T, galectin-3 and C-terminal propeptide of type I procollagen at long term follow-up in heart failure patients with reduced ejection fraction: Comparison with soluble AXL and BNP. *Int J Cardiol* 2016, 225:113-119.
62. Lee YJ, Han JY, Byun J, Park HJ, Park EM, Chong YH, Cho MS, Kang JL: Inhibiting Mer receptor tyrosine kinase suppresses STAT1, SOCS1/3, and NF-kappaB activation and enhances inflammatory responses in lipopolysaccharide-induced acute lung injury. *J Leukoc Biol* 2012, 91(6):921-932.
63. Zagorska A, Traves PG, Lew ED, Dransfield I, Lemke G: Diversification of TAM receptor tyrosine kinase function. *Nat Immunol* 2014, 15(10):920-928.

Figures

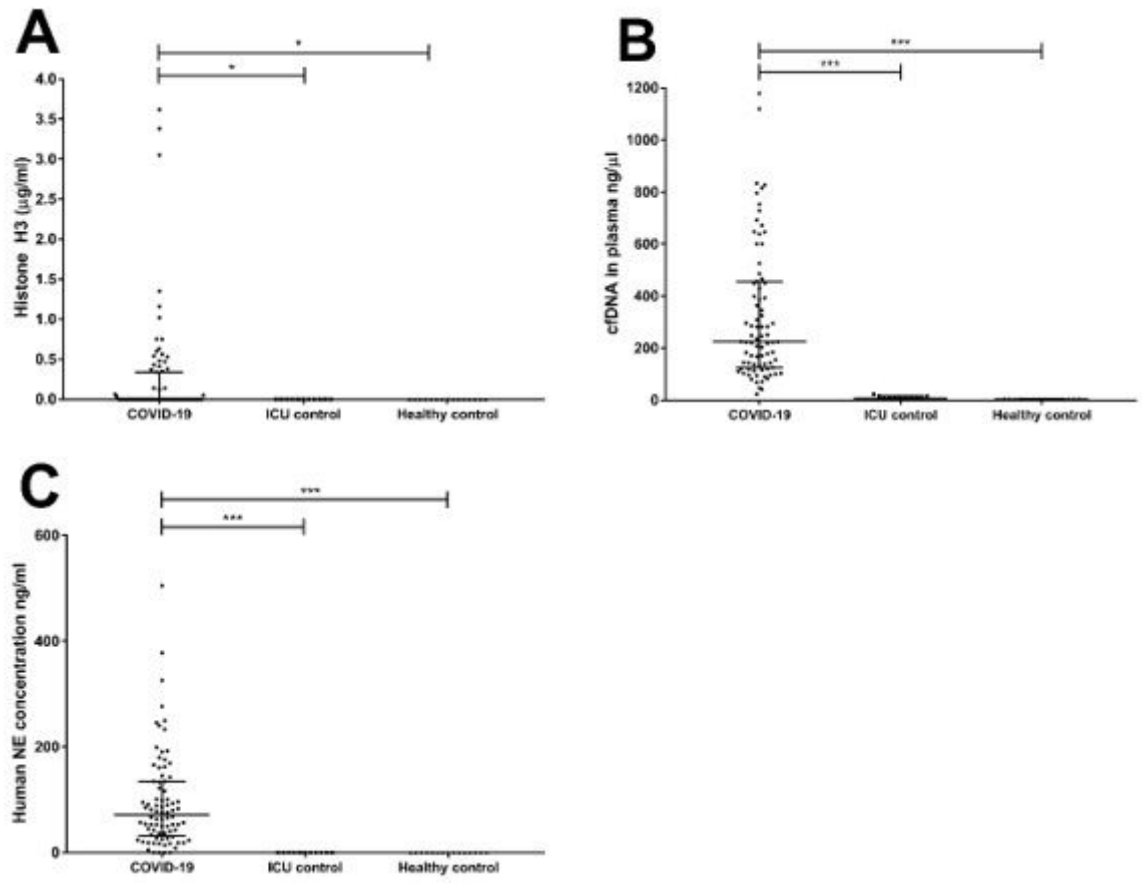

Figure 1

Detection of plasma markers H3, cfDNA and NE. Plasma from COVID-19 ICU patients (n=83) and non-COVID-19 ICU patients (n=11) was tested for the presence of extracellular histone H3 (A), cfDNA (B) and neutrophil elastase (C) at ICU admission. P-values were calculated with the Kruskall-Wallis test with Dunn's post-hoc test. P-values were considered significant if p < 0.05, * 0.05, ** 0.01, *** 0.001

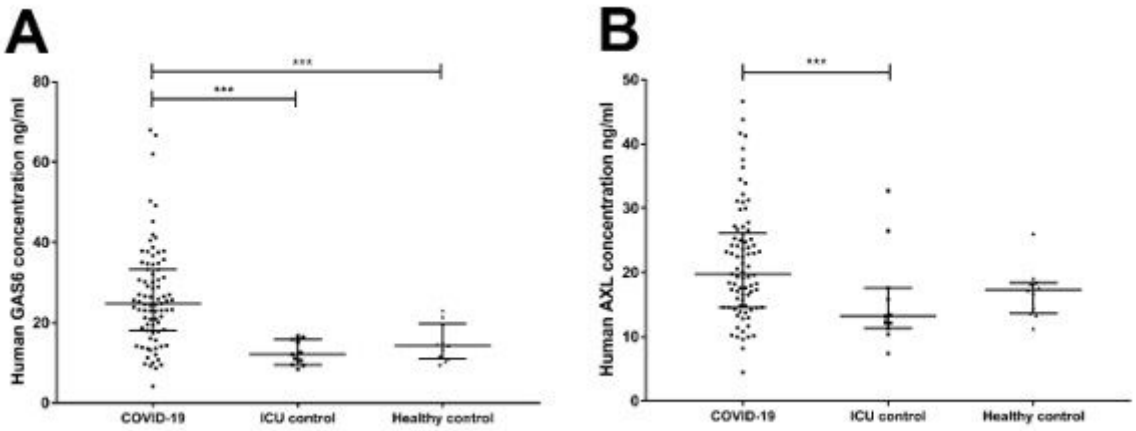

Figure 2

Detection of plasma markers GAS6 and sAXL. Plasma from COVID-19 ICU patients (n=83) and non-COVID-19 ICU patients (n=11) was tested for the presence of GAS6 (A), sAXL (B) at ICU admission. P-values were calculated with the Kruskall-Wallis test with Dunn's post-hoc test. P-value were considered significant if p < 0.05, * 0.05, ** 0.01, *** 0.001.

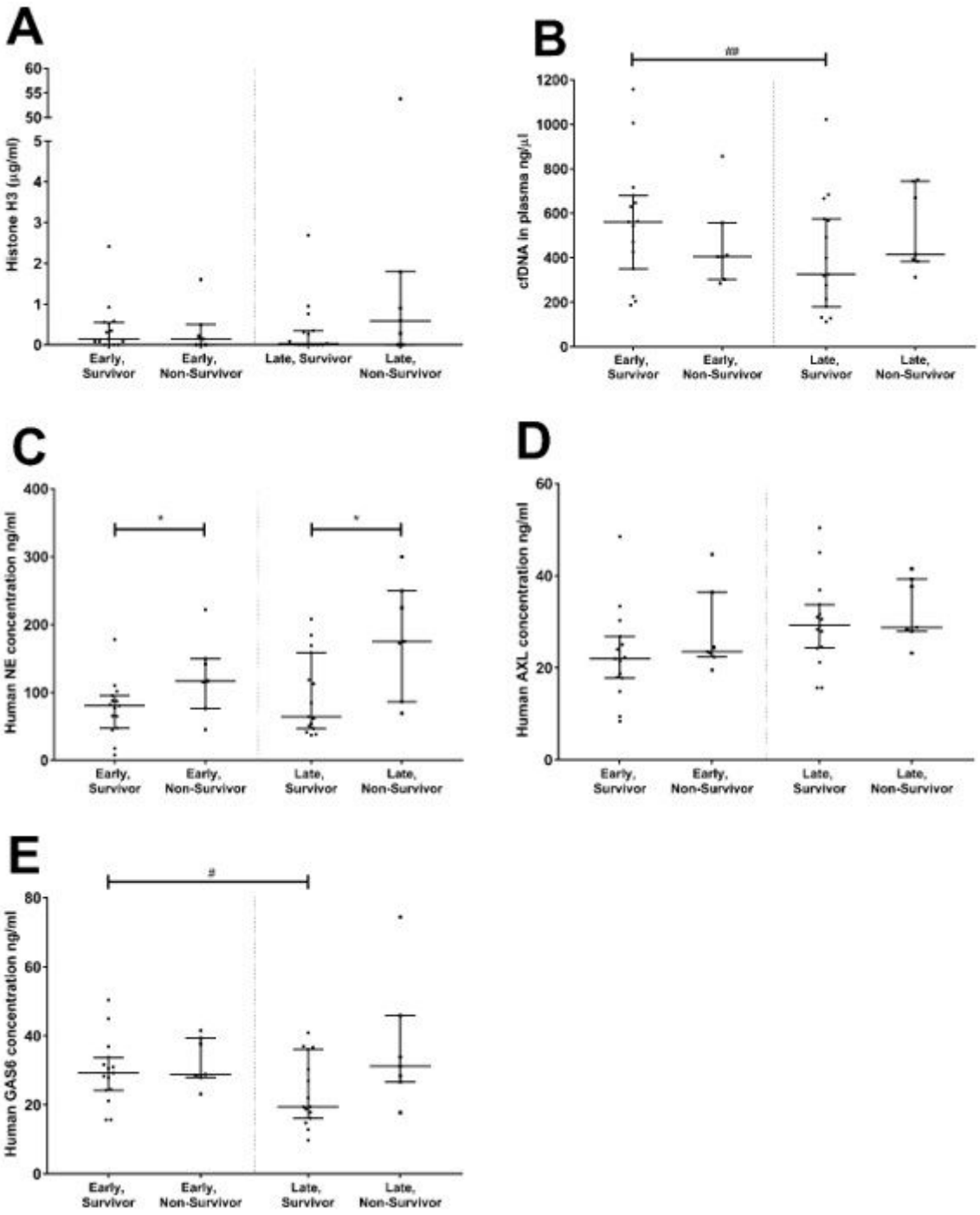

Figure 3

Detection of plasma markers GAS6 and sAXL. Plasma from COVID-19 ICU patients (n=83) and non-COVID-19 ICU patients (n=11) was tested for the presence of GAS6 (A), sAXL (B) at ICU admission. P-

values were calculated with the Kruskall-Wallis test with Dunn's post-hoc test. P-value were considered significant if p < 0.05, * 0.05, ** 0.01, *** 0.001.

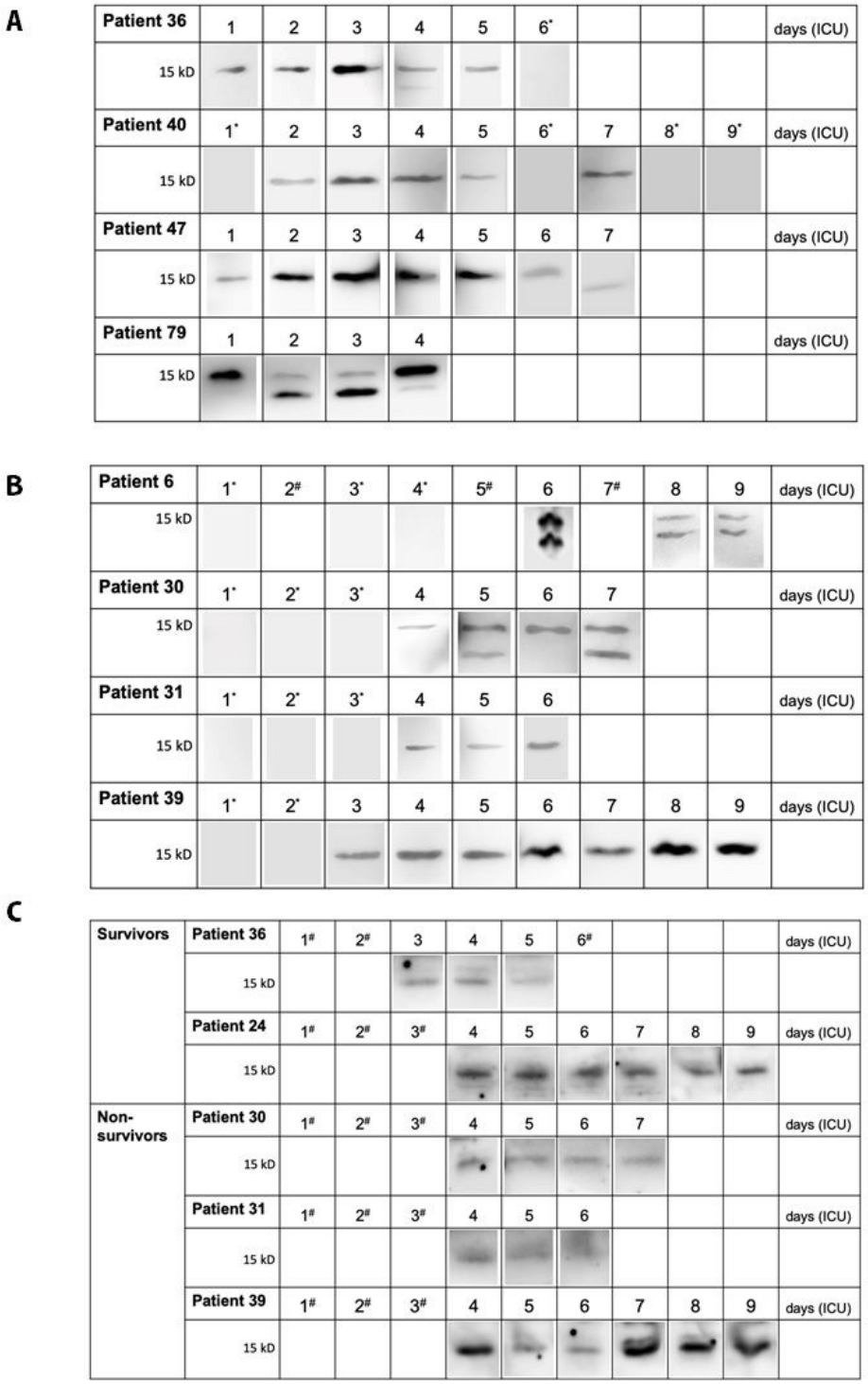

Figure 4

Western blot analysis of COVID-19 patient plasma. Plasma dilutions were run on SDS-PAGE and histone H3 was detected using a primary anti-H3 antibody. Along with patient plasma, aliquots of purified human histone H3 were run for comparison and quantitation by means of fluor imaging. Full length histone H3 is

visible at 15 kDa and cleaved histone H3 at 12 kDa. Results are shown as a composite of different blots. Multiple day follow-up examples are given for (A) COVID-19 survivors (B) COVID-19 non-survivors (C) examples of the randomly selected H3 positive samples for citrullination analysis. *no histone H3 detected that day, #plasma samples not provided

Supplementary Files

This is a list of supplementary files associated with this preprint. Click to download.

- SupplementaryTables.docx